Journal of Nuclear Materials 307–311 (2002) 1088–1092
journal of nuclear materials
www.elsevier.com/locate/jnucmat

Interfacial characterization of CVI-SiC/SiC composites

W. Yang [a,*], A. Kohyama [a,b], T. Noda [c], Y. Katoh [a,b], T. Hinoki [a], H. Araki [c], J. Yu [d]

[a] Institute of Advanced Energy, Kyoto University, Kyoto, Japan
[b] CREST-ACE, Japan Science and Technology Corporation, Japan
[c] National Research Institute for Metals, CREST, Tsukuba, Ibaraki, Japan
[d] China Institute of Atomic Energy, Beijing, China

Abstract

The mechanical properties of the interfaces of two families of chemical vapor infiltration SiC/SiC composites, advanced Tyranno-SA and Hi-Nicalon fibers reinforced SiC/SiC composites with various carbon and SiC/C interlayers, were investigated by single fiber push-out/push-back tests. Interfacial debonding and fibers sliding mainly occurred adjacent to the first carbon layer on the fibers. The interfacial debonding strengths and frictional stresses for both Tyranno-SA/SiC and Hi-Nicalon/SiC composites were correlated with the first carbon layer thickness. Tyranno-SA/SiC composites exhibited much larger interfacial frictional stresses compared to Hi–Nicalon/SiC composites. This was assumed to be mainly contributed by the rather rough surface of the Tyranno-SA fiber.

1. Introduction

There is a strong demand for high performance ceramic matrix composites for application in advanced energy systems, such as nuclear fusion reactors. SiC/SiC composites are considered to be the most potential candidates in the conceptual designs of fusion reactors [1]. It is well recognized that the quality of the fiber/matrix interface is one of the key roles for SiC/SiC composites [2]. Damage tolerance results from the deviation of matrix cracks into the interface. This phenomenon can be controlled through the deposition of a single coating or multiple coatings on the fibers. Carbon remains the most efficient interphase [3]. However, it is very sensitive to oxidation. Improving the oxidation resistance requires thinner carbon interphases while deviation of matrix cracks needs sufficient thickness of the interphases. Recently, an alternative multiple interphase, $(PyC–SiC)_n$, has been developed [4]. Improved oxidation resistance of the multilayers is expected by sufficient thickness of the carbon sub-layer.

In the previous work, the flexural properties of 2D plain-woven chemical vapor infiltration (CVI)-Hi-Nicalon^{TM}/SiC composites with various carbon and SiC/C layers were studied [5]. The results indicated strong influences of the layers on the materials properties. Recently, another family of SiC/SiC composites, advanced Tyranno-SA fiber (2D plain-woven) reinforced CVI-SiC/SiC composites, have been developed and the tensile performance upon unloading–reloading cycles was investigated [6]. These results indicated strong interfaces in these composites.

The primary objective of this study is to extract the interfacial debonding strength (IDS) and frictional stress (IFS) of the two families of SiC/SiC composites using single fiber push-out/push-back tests. The influences of the layers and fibers surface roughness have been investigated, too.

* Corresponding author. Address: Nano-Materials Laboratory, National Institute for Materials Science, Nano-Fabrication Research Group, 1-2-1 Sengen, Tsukuba, Ibaraki 305-0047, Japan. Tel.: +81-774 38 3465/+81-298 59 2739; fax: +81-774 38 3467/+81-298 59 2701.

E-mail addresses: wenyang@iae.kyoto-u.ac.jp, yang.wen@nims.go.jp (W. Yang).

0022-3115/02/$ - see front matter © 2002 Elsevier Science B.V. All rights reserved.
PII: S0022-3115(02)00949-2

2. Experimental

2.1. Materials

The composites and their porosities and interlayer structures investigated in this study are given in Table 1. Detailed information about the composites fabrication and layers examination is published elsewhere [5,6]. Composites with initial T in the specimen I.D. in Table 1 are reinforced with 2D as-received Tyranno-SA fabrics and those with initial H are reinforced with 2D as-received Hi-Nicalon fabrics.

2.2. Single fiber push-out/push-back tests

Single fiber push-out/push-back tests were carried out to extract the IDS and IFS, respectively, using a load controlled micro-indentation testing system with a triangular diamond pyramidal indenter. The specimens were carefully ground and polished with a final polish diamond paste (with the grain size of 1 μm). The detailed push-out/push-back test procedure was described elsewhere [7]. About 20 push-out and 15 push-back tests were conducted for each specimen. Both IDS and IFS were defined by

$$S = P/Dt,$$

where P is the push-out/push-back loads [7]. D and t are the fiber diameter and specimen thickness. The pushed and popped fibers as well as interfacial debondings were examined by field emission scanning electron microscopy using JEOL JSM-6700F.

3. Results and discussion

Fig. 1 shows typical push-out/push-back load–indenter displacement curves obtained in this study.

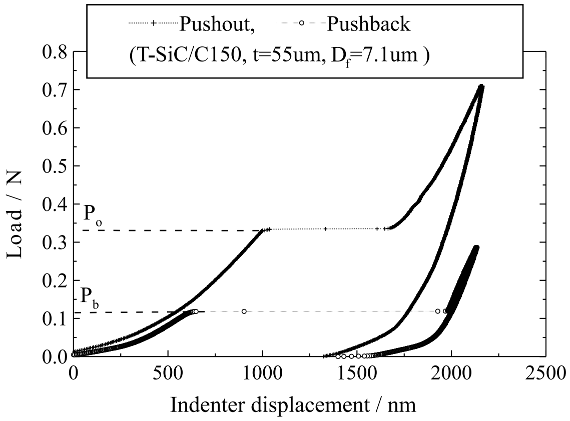

Fig. 1. Representative single fiber push-out/push-back load–displacement curves.

Each step of the curves has been explained in detail by Hinoki [7]. The push-out load, P_o in the figure, is essentially the load for fiber debonding and sliding as well as contributions from fiber elastic/plastic deformation and Poisson expansion effects. The push-back load, P_b in the figure, is mainly used to initiate the sliding of the debonded fiber. In the present study, P_o and P_b are used to define the IDS and IFS, respectively.

Fig. 2 shows the SEM image of a push-back fiber after a push-out test in the specimen from composite T-SiC/C150, in which a SiC layer of 150 nm thickness was deposited on the fibers prior to the deposition of a 150 nm carbon layer. Fig. 2 shows that the SiC layer was pushed out together with the fiber while the carbon layer remained in the matrix. This indicates that debonding and sliding occurred at the interface between carbon and SiC layers during the push-out and push-back tests. Similar behaviors were observed in the specimen from another SiC/C layered Tyranno-SA/SiC composite,

Table 1
The SiC/SiC composites and interfacial debonding/frictional stresses

Specimen I.D.	Interlayer structure and thickness[a] (nm)	Porosity (%)	Specimen thickness (μm)	IDS[a] (MPa)	IFS[a] (Pa)
T-NL	F/M	10.6	33	>633	–
T-C50	F/C$^{50\ (8)}$/M	20.4	80	331 (140)	63 (28)
T-C100	F/C$^{100\ (19)}$/M	15.1	35	342 (97)	161 (40)
T-C200	F/C$^{200\ (34)}$/M	14.6	111	195 (51)	98 (39)
T-SiC/C80	F/SiC$^{150\ (23)}$/C$^{80\ (15)}$/M	16.4	73	414 (117)	149 (64)
T-SiC/C150	F/SiC$^{150\ (25)}$/C$^{150\ (28)}$/M	21.8	55	284 (96)	101 (38)
H-NL	F/M	15.8	34	505 (91)	49 (14.3)
H-C150	F/C$^{150\ (21)}$/M	15.3	60	212 (33)	26 (7.1)
H-C220	F/C$^{220\ (31)}$/M	17.4	55	121 (31)	21 (6.9)
H-C760	F/C$^{760\ (116)}$/M	17.9	76	71 (31)	18 (6.4)
H-SiC/C380	F/SiC$^{250\ (42)}$/C$^{380\ (57)}$/M	18.4	89	81 (14)	37 (7.4)
H-C80/SiC/C	F/C$^{80\ (13)}$/SiC$^{150\ (25)}$/C$^{70\ (16)}$/M	15.3	58	103 (10)	13 (3.3)

[a] Included in parentheses are the standard deviations.

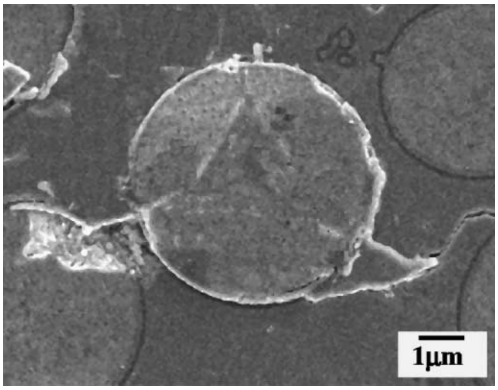

Fig. 2. SEM image of a push-back fiber of composite T-SiC/C150.

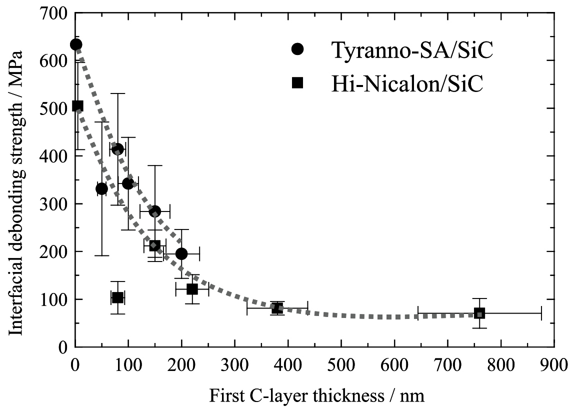

Fig. 3. The first carbon layer thickness dependence of the IDS.

namely T-SiC/C80. Debonding and fiber sliding were found to always take place at the fiber/carbon interfaces for single carbon layered Tyranno-SA/SiC composites. For the Hi-Nicalon/SiC composites, debonding and sliding occurred mostly along the very fiber surfaces, with occasional debonding at the SiC/C layers interfaces in the composite H-SiC/C380. The first layer on the fibers in this composite is SiC. However, three-point bending [5] and recycle tensile tests [8] revealed interfacial debonding and fiber sliding mostly at the SiC/C layers interfaces in this composite. SEM examination revealed that for both composite families, debonding and fiber sliding always occurred at the fiber/interlayer interfaces when carbon was first deposited on the fibers. A first SiC layer on the fibers seems likely to move the fiber/matrix debonding to the SiC/C layers interface.

3.1. Interfacial debonding and frictional stresses

The IDS and IFS values of the composites derived from the push-out/push-back curves are summarized in Table 1. A wide range of IDS, from 71 to >633 MPa, was obtained. Both IDS and IFS of Tyranno-SA/SiC composites are larger than that of Hi-Nicalon/SiC composites, especially for the IFS.

3.2. Influence of first carbon layer thickness

As discussed before, interfacial debonding and fiber sliding seem to take place mostly at the interface adjacent to the first carbon layers in both composite families. Rebillat et al. [3] has reported that the interfacial characteristics seemed to be related to the thickness of the first carbon layer on the fibers in as-received Nicalon fiber reinforced CVI-SiC/SiC composites with (C-SiC)$_n$ interlayers [3]. Therefore, the IDS and IFS in this study, are correlated with the first carbon layer on the fibers. Fig. 3 shows the IDS of Tyranno-SA/SiC and Hi-Nicalon/SiC versus the first carbon layers thickness. Both composite families exhibit a strong carbon layer thickness dependence of the IDS. The IDS of Tyranno-SA/SiC decreased quickly from over 633 to 195 MPa with increasing the carbon layer thickness up to 200 nm. A similar trend is as well demonstrated by the Hi-Nicalon/SiC composites. In case the carbon layer is thicker than 200 nm, the Hi-Nicalon/SiC composites exhibit almost stable IDS. This suggests that no significant influence on the IDS is provided by the carbon in the carbon layers beyond 200 nm for Hi-Nicalon/SiC composites. Fig. 3 indicates lower IDS of composite H-C80/SiC/C. SEM examination of the specimen revealed a large amount of fibers, which were pre-debonded, likely due to some damages of the interface near the polished surface during the cut and polishing process.

Regarding the IFS of the two composite families to the first carbon layer thickness revealed similar trends as that of IDS, as shown in Fig. 4. The IFS of Tyranno-SA/SiC is substantially larger than that of Hi-Nicalon/SiC, with the highest value of 161 MPa achieved by

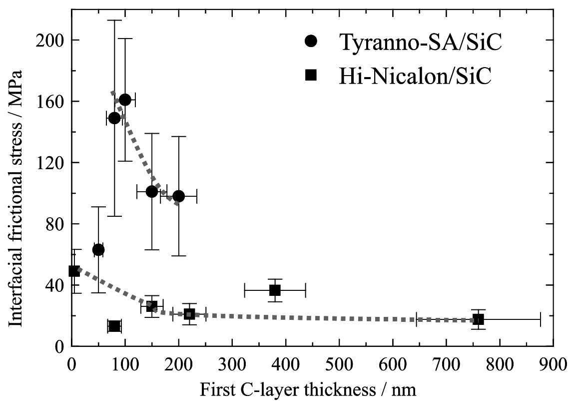

Fig. 4. The first carbon layer thickness dependence of the IFS.

composite T-C100. Among the Hi-Nicalon/SiC composites with interlayers, the highest IFS was obtained by the composite H-SiC/C380, although 380 nm thick carbon was applied. This indicates that the deposition of SiC layers on as-received Hi-Nicalon fiber might increase the composite IFS. No effect like this was noticed in the Tyranno-SA/SiC composites. Fig. 4 shows that almost no further decrease of the IFS of Hi-Nicalon/SiC composites occurred when the carbon is thicker than 200 nm.

3.3. Influence of fiber surface roughness

Interfacial roughness has been shown to contribute substantially to the interfacial friction [9]. Fig. 5 shows the SEM images of the surfaces of the Tyranno-SA and Hi-Nicalon fibers. It is obvious that the surface of Tyranno-SA fiber is much rougher compared to that of Hi-Nicalon fiber. In SiC/SiC composites, the radial thermal residual stresses on the fibers and the stresses induced by the fiber surface roughness during fiber sliding can be described with the equations from Jero et al. [9]:

$$\sigma_r^N = \kappa(\alpha_m^r - \alpha_f^r)\Delta T + \kappa\left(\frac{\delta}{R_f}\right),$$

where

$$\kappa = \frac{E_m E_f}{E_m(1 - \upsilon_f^r) + E_f(1 + \upsilon_m^r)}.$$

α_m^r and α_f^r are the coefficients of thermal expansions (CTE) of the fiber and matrix in radial direction, respectively, as given in Table 2. T is the temperature difference between fabrication (1273 K) and push-out/push-back tests (293 K). δ is the fiber surface roughness amplitude given in Fig. 5. R_f is the fiber radius. E_f, E_m, υ_f^r and υ_m^r are Young's moduli and Poisson's ratios of the fiber and matrix. Since the Tyranno-SA fiber is essentially a high-crystallized stoichiometric SiC fiber [10], the Poisson's ratio and CTE are considered as the same of chemical vapor deposition (CVD) SiC. The effects of fiber texture and volume fraction in the composites are neglected in this study.

Table 2
Some properties of the fibers and matrix

	E (GPa)	R_f (μm)	$\upsilon_{f,m}^r$	$\alpha_{f,m}^r \times 10^{-6}$ [a] (K^{-1})
Tyranno-SA	410	3.75	0.21	4.6
Hi-Nicalon	270	7.5	0.12	3.5
CVD-SiC	450		0.21	4.6

[a] RT to 773 K.

The radial thermal residual stresses were calculated to be zero for T-NL and 185 MPa for H-NL with the fibers under compression. Stresses induced by the fiber surface roughness are 219 and 30 MPa in Tyranno-SA/SiC and Hi-Nicalon/SiC composites, respectively. The stress induced by the fiber surface roughness in Tyranno-SA/SiC is much higher than that in Hi-Nicalon/SiC. It is even higher than the total stresses, consisting of thermal residual stress and fiber surface roughness misfit stress in the latter. Therefore, the large IFS of Tyranno-SA/SiC composites are believed to be mainly due to the rougher surface of the Tyranno-SA fibers. The relatively higher IFS of H-SiC/C380 (see Fig. 4) is likely due to a rougher fiber sliding surface between the SiC and the carbon layers [8].

4. Summary

The interfacial debonding strength and frictional stress of Tyranno-SA/SiC and Hi-Nicalon/SiC composites with various SiC/C interlayers have been investigated using single fiber push-out/push-back tests. Several conclusions can be summarized: (1) The IDS and IFS of the two families of CVI-SiC/SiC composites are

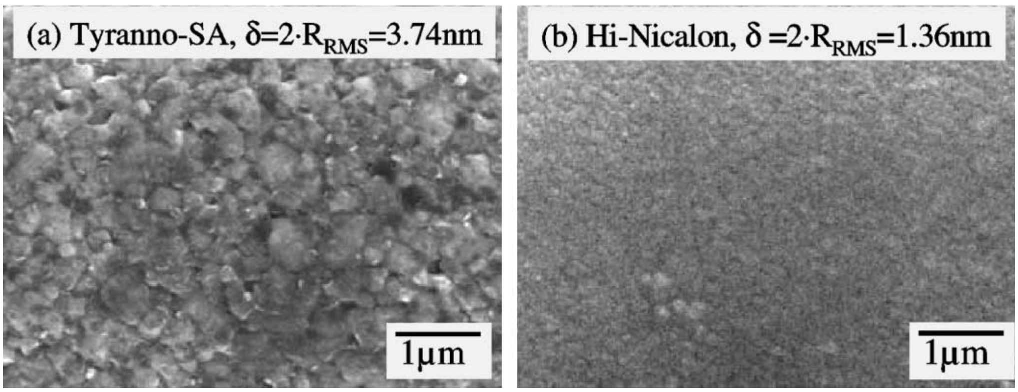

Fig. 5. Roughness of (a) Tyranno-SA and (b) Hi-Nicalon fiber surfaces (SEM micrographs). R_{RMS} means root-mean-square [7].

obtained and quantitatively related to the first carbon layer thickness. (2) A first SiC layer on the fibers demonstrates the ability to control the fiber/matrix debonding within the SiC/C multilayers rather than on the very fiber surface. (3) Large IFS is exhibited by Tyranno-SA/SiC composites. This is mainly attributed to the rough surface of the Tyranno-SA fiber.

References

[1] A. Kohayam, M. Seki, K. Abe, T. Muroga, H. Matsui, S. Jitsukawa, S. Matsuda, J. Nucl. Mater. 283–287 (2000) 20.
[2] T.M. Besmann, D.P. Stinton, E.R. Kupp, S. Shanmugham, P.K. Liaw, J. Mater. Res. Soc. Symp. Proc. 458 (1997) 147.
[3] F. Rebillat, J. Lamon, R. Naslain, E. Lara-Curzio, M.K. Ferber, T.M. Besmann, J. Am. Ceram. Soc. 81 (9) (1998) 2315.
[4] R. Naslain, in: A.G. Evans, R. Naslain (Eds.), High-Temperature Ceramic–Matrix Composites II: Manufacturing and Materials Development, Ceramic Transactions, vol. 58, American Ceramic Society, Westerville, OH, 1995, p. 23.
[5] W. Yang, H. Araki, T. Noda, J.Y. Park, Y. Katoh, T. Hinoki, J. Yu, A. Kohyama, Mater. Trans. 43 (10) (2002), in press.
[6] W. Yang, A. Kohyama, T. Noda, Y. Katoh, H. Araki, J. Yu, J. Am. Ceram. Soc., submitted.
[7] T. Hinoki, Investigation of mechanical properties and microstructure of SiC/SiC composites for nuclear application, Doctoral thesis, Institute of Advanced Energy, Kyoto University, 2001.
[8] T. Hinoki, W. Yang, T. Nozawa, T. Shibayama, Y. Katoh, A. Kohyama, J. Nucl. Mater. 289 (2001) 23.
[9] P.D. Jero, R.J. Kerans, T.A. Parthasarathy, J. Am. Ceram. Soc. 74 (11) (1998) 2793.
[10] T. Ishikawa, Y. Kohtoku, K. Kumagawa, T. Yamamura, T. Nagasawa, Nature 391 (6669) (1998) 773.